Journal of Zhejiang University-SCIENCE C (Computers & Electronics)
ISSN 1869-1951 (Print); ISSN 1869-196X (Online)
www.zju.edu.cn/jzus; www.springerlink.com
E-mail: jzus@zju.edu.cn

Differential multiuser detection using a novel genetic algorithm for ultra-wideband systems in lognormal fading channel*

Zheng-min KONG[†1,2], Liang ZHONG[2,3], Guang-xi ZHU[†‡2,3], Li DING[1]

([1]*Department of Automation, Wuhan University, Wuhan 430072, China*)

([2]*Wuhan National Laboratory for Optoelectronics, Huazhong University of Science & Technology, Wuhan 430074, China*)

([3]*Department of Electronics and Information Engineering, Huazhong University of Science & Technology, Wuhan 430074, China*)

[†]E-mail: kongzhengmin5@163.com; gxzhu@126.com

Received July 21, 2010; Revision accepted Dec. 6, 2010; Crosschecked July 29, 2011

Abstract: We employ a multiuser detection (MUD) method using a novel genetic algorithm (GA) based on complementary error function mutation (CEFM) and a differential algorithm (DA) for ultra-wideband (UWB) systems. The proposed MUD method is termed CEFM-GA DA for short. We describe the scheme of CEFM-GA DA, analyze its algorithm, and compare its computational complexity with other MUDs. Simulation results show that a significant performance gain can be achieved by employing the proposed CEFM-GA DA, compared with successive interference cancellation (SIC), parallel interference cancellation (PIC), conventional GA, and CEFM-GA without DA, for UWB systems in lognormal fading channel. Moreover, CEFM-GA DA not only reduces computational complexity relative to conventional GA and CEFM-GA without DA, but also improves bit error rate (BER) performance.

Key words: Multiuser detection (MUD), Ultra-wideband (UWB), Genetic algorithm (GA), Complementary error function mutation (CEFM), Differential algorithm (DA)

doi:10.1631/jzus.C1000257 **Document code:** A **CLC number:** TN929.5

1 Introduction

The recent increase in demand for short-range and very high data transmission rates in wireless communications has prompted the development of a new generation of broadband wireless communication systems, namely ultra-wideband (UWB) systems (Qiu, 2005; Shen *et al.*, 2006a; 2006b; Ahmadi-Shokouh and Qiu, 2009). A UWB system utilizes a frequency spectrum between 3.1 GHz and 10.6 GHz, with a channel bandwidth which is greater than 500 MHz or 20% of the center frequency. It has a transmission power level below the Federal Communications Commission (FCC) limit on spurious emissions (<−41.3 dBm/MHz) (ECMA International, 2008). The characteristics of huge bandwidth and low transmission power have made UWB technology become a new focus in both the academic and industrial sectors.

Interest in the study of UWB systems has increased, especially the development of multiuser detection (MUD) techniques in such systems. The well-known MUD technique, which originates from code division multiple access (CDMA) systems, can also be applied in the context of multiple access UWB systems to combat multiple access interference (MAI) and improve the system performance. The optimal multiuser detector proposed by Verdu (1998) had high computational complexity and was too expensive to handle. Therefore, suboptimal detectors have become a focus of research. For example, a minimum mean square error (MMSE) method was investigated by Li and Rusch (2002) and Kaligineedi and Bhargava

‡ Corresponding author

* Project supported by the National High-Tech R & D Program (863) of China (Nos. 2008AA01Z204 and 2009AA011202), the Key National Science & Technology Specific Projects (Nos. 2009ZX03003-003-2, 2009AA01Z205, 2009ZX03002-009, and 2010ZX03003-001-2), and the National Natural Science Foundation of China (No. 60802009)

(2008) to compute filter weights and deal with frequency-domain equalization, respectively, for MUD in UWB systems. An interference cancellation (IC) technique was developed by Boubaker and Letaief (2004) in direct sequence UWB (DS-UWB) systems. Adaptive MUDs based on the recursive least square (RLS) principles were operated by Biradar *et al*. (2008) and Ahmed and Yang (2010). However, the bit error rate (BER) of the system is high when suboptimal detection techniques, like conventional IC (Boubaker and Letaief, 2004), are used in UWB systems. These conventional detectors are not good enough for UWB systems. Thus, exploiting intelligent computation techniques would seem to be a better approach for obtaining improved BER performance. Among the intelligent computation techniques, genetic algorithm (GA) is the most popular method for engineering optimization. Tan *et al*. (2006) presented a conventional GA MUD algorithm for UWB channel. Wen *et al*. (2010) developed a GA-based hybrid detection for MUD in UWB systems. However, the BER performance and computational complexity of conventional GA-based MUD remain to be improved in UWB systems.

In this paper, we propose a MUD method based on a novel GA with complementary error function mutation (CEFM) and a differential algorithm (DA) for UWB systems in lognormal fading channel (Saleh and Valenzuela, 1987; Foerster, 2003; Ahmadi-Shokouh and Qiu, 2009), namely CEFM-GA DA. Compared with conventional GA (Tan *et al.*, 2006; Surajudeen-Bakinde *et al.*, 2009; Wen *et al.*, 2010) and IC (Boubaker and Letaief, 2004) multiuser detectors in UWB systems, our novel GA, which is based upon CEFM, improves the mutation process to achieve a better BER performance. Moreover, using our proposed DA a good BER performance can be obtained at a relatively low computational complexity. In other words, our proposed CEFM-GA DA MUD not only improves BER performance, but also reduces computational complexity.

2 System model

2.1 Transmission model

We consider a K-user model for a synchronous DS-UWB communication system over indoor multipath channel, where each user uses a unique spreading sequence. The transmitted signal generated by the kth user is given by

$$x_k(t)=\sqrt{E_k}b_k s_k(t), \tag{1}$$

where E_k is the kth user's signal energy per bit, b_k is the kth user's data modulated by binary phase shift keying (BPSK), and $s_k(t)$ is the kth user's spreading waveform which is given by

$$s_k(t)=\frac{1}{\sqrt{N_\mathrm{s}}}\sum_{i=1}^{N_\mathrm{s}}c_k(i)p(t-iT_\mathrm{c}), \tag{2}$$

where N_s is the length of the spreading sequence, $c_k(i)$ is the ith spreading code chip assigned to the kth user, T_c is the chip duration, and $p(t)$ is the second derivative of Gaussian pulse (Li and Rusch, 2002) given by

$$p(t)=[1-4\pi(t/\tau)]\exp[-2\pi(t/\tau)^2], \tag{3}$$

where τ is the pulse shape parameter.

2.2 UWB channel model

A UWB channel model, including cluster and ray phenomena (Saleh and Valenzuela, 1987; Molisch *et al.*, 2003), is very different from a narrowband wireless channel model. The distributions of the parameters of a UWB channel model on small-scale fading depend on environments and can include lognormal, Nakagami, or Rician fading distributions (Ahmadi-Shokouh and Qiu, 2009). Our past work (Zhong *et al.*, 2010) showed that lognormal fading UWB channel seems to suit better the Chinese office and laboratory environment. This lognormal fading distribution is the same as the distribution in the IEEE 802.15.3a indoor channel model (Molisch *et al.*, 2003). Thus, we consider a lognormal fading channel for the UWB indoor transmission environment. The channel impulse response (CIR) of the UWB channel of multipath mode for the kth user is as follows:

$$h_k(t)=X_k\sum_{l=0}^{L}\sum_{j=0}^{J}\alpha_{j,l}^k\delta(t-T_l^k-\tau_{j,l}^k), \tag{4}$$

where X_k represents the lognormal shadowing, T_l^k is the delay of the lth cluster, $\tau_{j,l}^k$ is the delay of the jth

multipath component (i.e., ray) relative to the lth cluster arrival time (i.e., T_l^k), and $\alpha_{j,l}^k$ are the multipath gain coefficients of the jth multipath component (i.e., ray) in the lth cluster. The coefficients $\alpha_{j,l}^k$ for the kth user can be defined as follows:

$$\alpha_{j,l}^k = p_{j,l}^k \xi_l^k \beta_{j,l}^k, \tag{5}$$

where $p_{j,l}^k$ is equiprobably 1 or -1 to show signal inversion because of reflections, and ξ_l^k and $\beta_{j,l}^k$ reflect the fading associated with the lth cluster and the jth ray of the lth cluster, respectively. Note that, $20\lg(\xi_l^k \beta_{j,l}^k) \propto N(\mu_{j,l}^k, \sigma_1^2 + \sigma_2^2)$ or $\left|\xi_l^k \beta_{j,l}^k\right| = 10^{(\mu_{j,l}^k + n_1 + n_2)/20}$, where $n_1 \propto N(0, \sigma_1^2)$ and $n_2 \propto N(0, \sigma_2^2)$ are independent and correspond to the fading on each cluster and ray, respectively.

$$E\left[\left|\xi_l^k \beta_{j,l}^k\right|^2\right] = \Omega_0 \mathrm{e}^{-T_l^k/\Gamma} \mathrm{e}^{-\tau_{j,l}^k/\gamma}, \tag{6}$$

where Ω_0 is the mean energy of the first path of the first cluster, and Γ and γ are the cluster decay factor and ray decay factor, respectively. Observing the above equations, $\mu_{j,l}^k$ can be calculated as

$$\mu_{j,l}^k = \frac{10\ln\Omega_0 - 10T_l^k/\Gamma - 10\tau_{j,l}^k/\gamma}{\ln 10} - \frac{(\sigma_1^2 + \sigma_2^2)\ln 10}{20}, \tag{7}$$

where σ_1 and σ_2 are the standard deviations of the cluster lognormal fading term and the ray lognormal fading term, respectively. The illustrations above show that the channel coefficients of multipath gain $\{\alpha_{j,l}^k\}$ fit a lognormal distribution.

There are two more parameters of the channel model, the cluster arrival rate Λ and the ray arrival rate λ (i.e., the arrival rate of path within each cluster), which are able to express the distributions of the cluster arrival time and the ray arrival time, respectively:

$$p(T_l^k \mid T_{l-1}^k) = \Lambda \exp[-\Lambda(T_l^k - T_{l-1}^k)], \quad l > 0, \tag{8}$$

$$p(\tau_{j,l}^k \mid \tau_{(j-1),l}^k) = \lambda \exp[-\lambda(\tau_{j,l}^k - \tau_{(j-1),l}^k)], \quad j > 0. \tag{9}$$

Finally, the total received signal can be obtained by

$$r(t) = \sum_{k=1}^{K} x_k(t) \otimes h_k(t) + n(t), \tag{10}$$

where $\otimes$ denotes linear convolution and $n(t)$ is the zero-mean additive white Gaussian noise (AWGN).

3 Differential multiuser detection using a genetic algorithm based on complementary error function mutation

GA is a probabilistic search technique based on the principle of biological evolution. Just as a biological organism evolves to more fully adapt to its environment, GA follows a path of analysis from which a design evolves, one that is optimal for the environmental restrictions placed upon it. GA uses probabilistic transition rules to select someone to reproduce or to die so as to guide their search toward regions of the search space with likely improvement (Gen and Cheng, 2000). Thus, GA is a powerful and globally stochastic search and optimization technique, and is widely employed in optimization problems of industrial engineering.

In this section, we discuss a novel GA based on CEFM aided MUD, and its DA for both further improvement of system BER performance and reduction of computational complexity.

3.1 Genetic algorithm based on complementary error function mutation

First, we define the trial data vector in our proposed GA based on CEFM (i.e., CEFM-GA) MUD as $\hat{\boldsymbol{b}} = [\hat{b}_1, \hat{b}_2, \cdots, \hat{b}_K]^{\mathrm{T}}$ for K users. Then,

$$\hat{r}(t) = \sum_{k=1}^{K} \sqrt{E_k}\, \hat{b}_k s_k(t) \otimes h_k(t) \tag{11}$$

represents the estimated value of the received signal $r(t)$ for K users.

Fig. 1 shows a flow chart of the proposed CEFM-GA assisted MUD used in the UWB system. After our proposed CEFM-GA MUD process, the trial datum $\hat{b}_k$ will be the optimum or near-optimum estimated value of the b_k in Eq. (1) for the kth user.

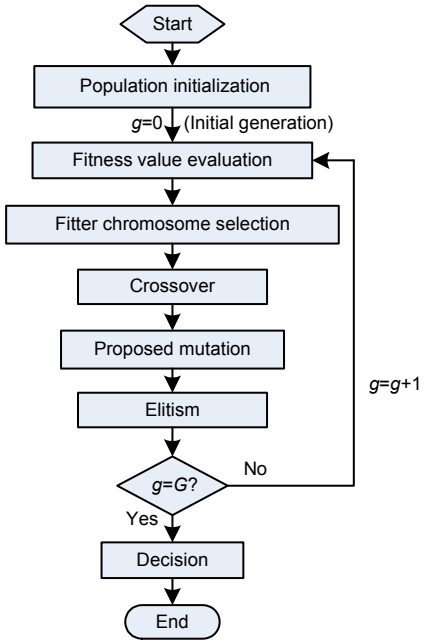

Fig. 1 Flow chart of the proposed CEFM-GA assisted multiuser detection scheme for UWB systems

For succinctness, we will simply describe the philosophy of the proposed CEFM-GA. Readers who are unfamiliar with GAs can refer to Goldberg (1989) or Gen and Cheng (2000) for details.

1. Start with encoding

For the start of the GA, the trial data vector $\hat{\boldsymbol{b}}$ must first be encoded into binary string form. The encoded binary string is regarded as a chromosome in GA and its elements are regarded as genes. Thus, the MUD can be treated as a multi-objective optimization solution that finds the most likely combination of the binary bits (Jiang *et al.*, 2006; Arifianto *et al.*, 2007).

Without loss of generality, BPSK modulation has already been employed in the transmission model. Thus, the chromosome encoding procedure is unnecessary. In this case, the number of genes in a chromosome, which is also the number of bits in a trial data vector for BPSK, is the number of users. If the transmission signals are modulated by QPSK, namely 2 bits per symbol, the chromosome must have 2-bit genes. In general, the number of bits in a symbol is equal to the number of bits in a gene.

2. Population initialization

After encoding, an initial population consisting of P members, called individuals, is created. In our proposed GA, each individual or chromosome in the population is represented by a vector including K bits. In the vector, each bit is a trial datum belonging to one of the K users. The pth individual which is the estimated value of $\boldsymbol{b}=[b_1,b_2,\cdots,b_K]^{\mathrm{T}}$ in Eq. (1) is defined as

$$\hat{\boldsymbol{b}}_p^{(g)}=[\hat{b}_{1,p}^{(g)},\hat{b}_{2,p}^{(g)},\cdots,\hat{b}_{K,p}^{(g)}]^{\mathrm{T}},\ p=1,\ 2,\ \ldots,\ P, \quad (12)$$

where superscript g (g=1, 2, …, G) denotes the gth generation and $\hat{b}_{k,p}^{(g)}$ denotes the kth (k=1, 2, …, K) gene of the pth individual at the gth generation.

After initialization of the population, the P individuals then begin the optimization process, in which the initial generation g is 1.

3. Fitness evaluation

In the procedure of this fitness evaluation, our GA exploits an objective function (OF) to evaluate the fitness of each individual in the population, which represents how closely each individual matches the optimum individual. Thus, the optimum individual can maximize the OF value. We will now discuss how to find the OF.

The solution of optimum detection is the most likely trial data vector $\hat{\boldsymbol{b}}_{\mathrm{opt}}$ that minimizes $\|r(t)-\hat{r}(t)\|_2$; that is,

$$\hat{\boldsymbol{b}}_{\mathrm{opt}}=\arg\left\{\min\left\|r(t)-\hat{r}(t)\right\|_2\right\}, \quad (13)$$

where $\hat{\boldsymbol{b}}_{\mathrm{opt}}\in\{\hat{\boldsymbol{b}}=[\hat{b}_1,\hat{b}_2,\cdots,\hat{b}_K]^{\mathrm{T}}\}$, $\hat{b}_k\in\{-1,1\}$, $k\in\{1,2,\ldots,K\}$, and $\|\cdot\|_2$ denotes Euclidean norm or Euclidean distance.

Next, we consider the likelihood function

$$f[r(t),0\le t\le T_{\mathrm{s}}\,|\,\hat{\boldsymbol{b}}]=\exp\left\{-\int_{T_{\mathrm{s}}}\left[r(t)-\hat{r}(t)\right]^2\mathrm{d}t/(2\sigma^2)\right\}. \quad (14)$$

Analyzing the differential part of the right hand side of Eq. (14), we find it to be an expression of the distance (Verdu, 1998). Observing Eqs. (13) and (14), the solution of optimum detection selects $\hat{\boldsymbol{b}}$ that can also maximize the likelihood function above (Verdu, 1998; Yen and Hanzo, 2004) or, ignoring the term which is independent of $\hat{\boldsymbol{b}}$ (i.e., $\int_{T_{\mathrm{s}}}r(t)^2\mathrm{d}t$), equivalently maximizes

$$\Omega(\hat{\boldsymbol{b}}) = 2\int_{T_s} \hat{r}(t)r(t)\mathrm{d}t - \int_{T_s} \hat{r}(t)^2\mathrm{d}t. \tag{15}$$

By substituting Eq. (11) into Eq. (15), we obtain

$$\begin{aligned}\Omega(\hat{\boldsymbol{b}}) = {} & 2\int_{T_s}\left[\sum_{k=1}^{K}\sqrt{E_k}\hat{b}_k s_k(t)\otimes h_k(t)\right]r(t)\mathrm{d}t \\ & -\int_{T_s}\left[\sum_{k=1}^{K}\sqrt{E_k}\hat{b}_k s_k(t)\otimes h_k(t)\right]^2\mathrm{d}t.\end{aligned} \tag{16}$$

Here, we define

$$S_k(t) = \sqrt{E_k}s_k(t)\otimes h_k(t)\,. \tag{17}$$

Then Eq. (16) can be rewritten as

$$\Omega(\hat{\boldsymbol{b}}) = 2\int_{T_s}\left(\sum_{k=1}^{K}\hat{b}_k S_k(t)\right)r(t)\mathrm{d}t - \int_{T_s}\left(\sum_{k=1}^{K}\hat{b}_k S_k(t)\right)^2\mathrm{d}t. \tag{18}$$

Substituting Eqs. (1) and (10) into Eq. (18), we obtain

$$\begin{aligned}&\Omega(\hat{\boldsymbol{b}}) \\ &= 2\int_{T_s}\left(\sum_{k=1}^{K}\hat{b}_k S_k(t)\right)\left(\sum_{k=1}^{K}\sqrt{E_k}b_k s_k(t)\otimes h_k(t)+n(t)\right)\mathrm{d}t \\ &\quad -\int_{T_s}\left(\sum_{k=1}^{K}\hat{b}_k S_k(t)\right)^2\mathrm{d}t \\ &= 2\int_{T_s}\left(\sum_{k=1}^{K}\hat{b}_k S_k(t)\right)\left(\sum_{k=1}^{K}b_k S_k(t)+n(t)\right)\mathrm{d}t \\ &\quad -\int_{T_s}\left(\sum_{k=1}^{K}\hat{b}_k S_k(t)\right)^2\mathrm{d}t \\ &= 2\int_{T_s}\left(\sum_{k=1}^{K}\hat{b}_k S_k(t)\right)\left(\sum_{k=1}^{K}b_k S_k(t)\right)\mathrm{d}t \\ &\quad +2\int_{T_s}\left(\sum_{k=1}^{K}\hat{b}_k S_k(t)\right)n(t)\mathrm{d}t - \int_{T_s}\left(\sum_{k=1}^{K}\hat{b}_k S_k(t)\right)^2\mathrm{d}t \\ &= 2\hat{\boldsymbol{b}}^{\mathrm{T}}\boldsymbol{S}\boldsymbol{S}^{\mathrm{T}}\boldsymbol{b} + 2\hat{\boldsymbol{b}}\boldsymbol{n} - (\hat{\boldsymbol{b}}^{\mathrm{T}}\boldsymbol{S})(\hat{\boldsymbol{b}}^{\mathrm{T}}\boldsymbol{S})^{\mathrm{T}} \\ &= 2\hat{\boldsymbol{b}}^{\mathrm{T}}\boldsymbol{R}\boldsymbol{b} + 2\hat{\boldsymbol{b}}\boldsymbol{n} - \hat{\boldsymbol{b}}^{\mathrm{T}}\boldsymbol{R}\hat{\boldsymbol{b}} \\ &= 2\hat{\boldsymbol{b}}^{\mathrm{T}}(\boldsymbol{R}\boldsymbol{b}+\boldsymbol{n}) - \hat{\boldsymbol{b}}^{\mathrm{T}}\boldsymbol{R}\hat{\boldsymbol{b}},\end{aligned} \tag{19}$$

where $\boldsymbol{n} = \int_{T_s} S_k(t)n(t)\mathrm{d}t$, and $\boldsymbol{R}=\boldsymbol{S}\boldsymbol{S}^{\mathrm{T}}$ is an auto and cross correlation matrix. We define $\boldsymbol{y}=\boldsymbol{R}\boldsymbol{b}+\boldsymbol{n}$, which can be treated as the output of the matched filter (MF). Thus, we treat $\Omega(\hat{\boldsymbol{b}})$ as the OF, which can be simplified as

$$\Omega(\hat{\boldsymbol{b}}) = 2\hat{\boldsymbol{b}}^{\mathrm{T}}\boldsymbol{y} - \hat{\boldsymbol{b}}^{\mathrm{T}}\boldsymbol{R}\hat{\boldsymbol{b}}. \tag{20}$$

Thus, the solution of optimum or near-optimum detection is the one that maximizes the OF value in Eq. (20), and $\boldsymbol{y}$ is the input of the proposed GA. The standard of fitness evaluation of the individuals is that the greater is the OF value of an individual, the fitter is the individual.

4. Selection

To evolve the population, some excellent individuals will be chosen to constitute a future population for reproduction. The fitter individuals with better genes are more likely to be selected to produce the offspring individuals (Goldberg, 1989). Thus, the rule of selection is based on their fitness or OF values (Jiang and Hanzo, 2007). The selection probability of the pth individual is

$$P_p = \frac{\Omega(\hat{\boldsymbol{b}}_p^{(g)}) - \Omega_{\mathrm{w}}^{(g)} + 1}{\sum_{p=1}^{P}(\Omega(\hat{\boldsymbol{b}}_p^{(g)}) - \Omega_{\mathrm{w}}^{(g)} + 1)}, \tag{21}$$

where $\Omega(\hat{\boldsymbol{b}}_p^{(g)})$ is the OF value of the pth individual at the gth generation, and $\Omega_{\mathrm{w}}^{(g)}$ is the worst OF value at the gth generation.

5. Crossover

Crossover is the operation by which the selected individuals exchange their genes to produce pairs of offspring. Concretely, the crossover operation randomly chooses one cutting point or many cutting points and exchanges the binary strings of individuals before or after the cutting point(s). For instance, after a cut in the first bit in each of the two strings 0011 and 1010, these two strings are crossed over to produce a new pair of offspring 0010 and 1011. Because the offspring inherit the merits of their parents, they are expected to be superior to their parents.

6. The proposed complementary error function mutation

To increase the diversity of the population, this mutation operation randomly changes some of the crossover results' genes. Without mutation, the GA's search falls into local optima. Thus, the mutation operation is crucial to the success of GA.

In this part, we present a new mutation operation, namely CEFM. In the proposed CEFM procedure, a

mutation probability $p_{\mathrm{m}}^{(i,j)}$ which is relative to a signal-to-noise ratio (SNR) from i to j is defined. It can be calculated with the help of a complementary error function (Proakis and Salehi, 2007)

$$\mathrm{erfc}(x)=\frac{2}{\sqrt{\pi}}\int_x^{\infty}\mathrm{e}^{-t^2}\mathrm{d}t,\quad x\geq 0. \tag{22}$$

Fig. 2 is an illustration of the mutation probability $p_{\mathrm{m}}^{(i,j)}$ for BPSK modulation. A vertical dashed line separates −1 and 1, and the Gaussian distribution $N(0, \sigma^2)$ is centered to the left side of that line, namely at the position of −1. Here, σ^2 is the noise variance at a specified SNR level. The mutation probability from −1 to 1 (i.e., $p_{\mathrm{m}}^{(-1,1)}$) is proportional to the shaded area in Fig. 2. It can be obtained by

$$p_{\mathrm{m}}^{(-1,1)}=\frac{1}{2}\mathrm{erfc}\left(\left|\frac{-1-1}{2}\right|\cdot\frac{1}{\sigma^2}\right)=\frac{1}{\sqrt{\pi}}\int_{\sigma^{-2}}^{\infty}\mathrm{e}^{-t^2}\mathrm{d}t. \tag{23}$$

Similarly, we can obtain

$$p_{\mathrm{m}}^{(1,-1)}=\frac{1}{2}\mathrm{erfc}\left(\left|\frac{1-(-1)}{2}\right|\cdot\frac{1}{\sigma^2}\right)=\frac{1}{\sqrt{\pi}}\int_{\sigma^{-2}}^{\infty}\mathrm{e}^{-t^2}\mathrm{d}t. \tag{24}$$

We find that $p_{\mathrm{m}}^{(-1,1)}=p_{\mathrm{m}}^{(1,-1)}$, and thus we define $p_{\mathrm{m}}=p_{\mathrm{m}}^{(-1,1)}=p_{\mathrm{m}}^{(1,-1)}$ as the CEFM probability for BPSK modulation.

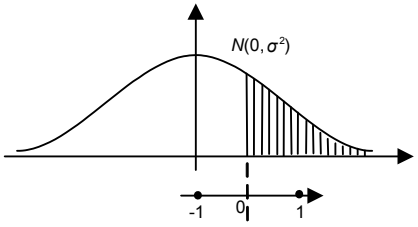

Fig. 2 Illustration of the mutation probability $p_{\mathrm{m}}^{(-1,1)}$ based on complementary error function mutation for BPSK

7. Elitism

An elitism operation (Fig. 1) is used to avoid losing excellent individuals which have higher fitness or greater OF values from one generation to another. The operation copies a small part of the best parent individuals, and replaces the worst offspring (Gen and Cheng, 2000).

8. Generation iteration

The genetic operations above are cycled from one generation to another, until the generation index g reaches its maximum G. If the number of generations G and/or the population size P are large enough, the final results of GA MUD for K users approach the optima (Hanzo and Keller, 2006; Jiang and Hanzo, 2007).

3.2 Differential algorithm for the proposed CEFM-GA MUD

The GA is convergent, but the degree of convergence depends on the number of generations G and/or the population size P (Jiang *et al.*, 2006; Wen *et al.*, 2010). As noted above, if P and/or G are sufficiently large, our CEFM-GA MUD approaches the optimum maximum likelihood detection results. However, increasing P and/or G increases the computational complexity of the MUD system. It is impractical to pursue a slightly higher degree of convergence or a slightly lower BER performance at the expense of much more computational complexity. Thus, we present a DA to solve the complexity problem. Besides the reduction of computational complexity, the DA can improve BER performance.

Fig. 3 shows the structure of the CEFM-GA with the DA. We exploit the DA in CEFM-GA to avoid unnecessary repeated calculations of certain terms in different generations. The kth user data $\boldsymbol{y}_k$ awaiting detection are forwarded to two CEFM-GA MUDs (Fig. 3). One CEFM-GA detector which has a large number of generations G_1 is the major detector while the other, which has a much smaller number of generations G_0, is an accessorial detector. The accessorial

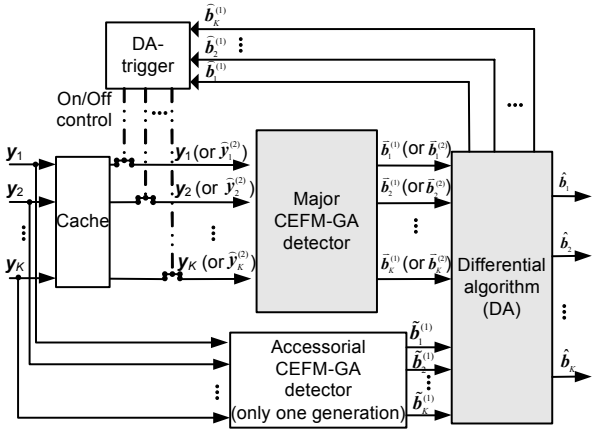

Fig. 3 Structure of the proposed CEFM-GA DA multi-user detector

CEFM-GA detector usually has few generations—one or two are enough. In our proposed DA, we consider one generation for the accessorial CEFM-GA detector. Let us analyze the principle of the DA. As mentioned in Eq. (20), the inputs of the major and accessorial CEFM-GA, which are the same, can be expressed as

$$\boldsymbol{y}=[\boldsymbol{y}_1, \boldsymbol{y}_2, \cdots, \boldsymbol{y}_K]^{\mathrm{T}}, \boldsymbol{y}_k=[y_k(1), y_k(2), ..., y_k(Q)], \quad (25)$$

where Q is the number of bits per packet, $k\in\{1, 2, ..., K\}$. The outputs of the major and accessorial CEFM-GA are different, and are respectively

$$\vec{\boldsymbol{b}}^{(1)}=[\vec{\boldsymbol{b}}_1^{(1)}, \vec{\boldsymbol{b}}_2^{(1)}, \cdots, \vec{\boldsymbol{b}}_K^{(1)}]^{\mathrm{T}},\ \vec{\boldsymbol{b}}_k^{(1)}=[\vec{b}_k^{(1)}(1), \vec{b}_k^{(1)}(2), ..., \vec{b}_k^{(1)}(Q)], \quad (26)$$

$$\tilde{\boldsymbol{b}}^{(1)}=[\tilde{\boldsymbol{b}}_1^{(1)}, \tilde{\boldsymbol{b}}_2^{(1)}, \cdots, \tilde{\boldsymbol{b}}_K^{(1)}]^{\mathrm{T}},\ \tilde{\boldsymbol{b}}_k^{(1)}=[\tilde{b}_k^{(1)}(1), \tilde{b}_k^{(1)}(2), ..., \tilde{b}_k^{(1)}(Q)], \quad (27)$$

where Q is the number of bits per packet, $k\in\{1, 2, ..., K\}$, and the superscript (1) denotes the first cycle of CEFM-GA detection. The DA (Fig. 3) defines a differential matrix

$$\begin{aligned}\hat{\boldsymbol{b}}^{(1)}&=\frac{\vec{\boldsymbol{b}}^{(1)}-\tilde{\boldsymbol{b}}^{(1)}}{2}=\left[\frac{\vec{\boldsymbol{b}}_1^{(1)}-\tilde{\boldsymbol{b}}_1^{(1)}}{2}, \frac{\vec{\boldsymbol{b}}_2^{(1)}-\tilde{\boldsymbol{b}}_2^{(1)}}{2}, ..., \frac{\vec{\boldsymbol{b}}_K^{(1)}-\tilde{\boldsymbol{b}}_K^{(1)}}{2}\right]^{\mathrm{T}}\\&=\begin{pmatrix}\dfrac{\vec{b}_1^{(1)}(1)-\tilde{b}_1^{(1)}(1)}{2} & \cdots & \dfrac{\vec{b}_1^{(1)}(Q)-\tilde{b}_1^{(1)}(Q)}{2}\\ \vdots & & \vdots\\ \dfrac{\vec{b}_K^{(1)}(1)-\tilde{b}_K^{(1)}(1)}{2} & \cdots & \dfrac{\vec{b}_K^{(1)}(Q)-\tilde{b}_K^{(1)}(Q)}{2}\end{pmatrix}\\&=[\hat{\boldsymbol{b}}_1^{(1)}, \hat{\boldsymbol{b}}_2^{(1)}, ..., \hat{\boldsymbol{b}}_K^{(1)}]^{\mathrm{T}}.\end{aligned} \quad (28)$$

Calculating the differential matrix $\hat{\boldsymbol{b}}^{(1)}$, we find that it contains many zeros, reflecting the convergence of the proposed GA, and that its non-zero elements are 1 or −1. The non-zero elements which result from the differences between $\vec{\boldsymbol{b}}^{(1)}$ and $\tilde{\boldsymbol{b}}^{(1)}$ reflect errors between the major and accessorial detectors, or a tendency for errors in the results of the CEFM-GA MUD (Nahler *et al*., 2002; Kong *et al*., 2008; 2010). For simplicity, we now focus our attention on the kth user. The DA saves $\hat{\boldsymbol{b}}_k^{(1)}$ ($k\in\{1, 2, ..., K\}$), and feeds it back to the DA-trigger (Fig. 3). According to the sequence $\hat{\boldsymbol{b}}_k^{(1)}$, the DA-trigger triggers $\boldsymbol{y}_k$, which is from the cache, and forms a new input $\hat{\boldsymbol{y}}_k^{(2)}$. Namely, when a non-zero signal in $\hat{\boldsymbol{b}}_k^{(1)}$ arrives, the DA-trigger (the initial state is connective) executes a trigger for a connection. Thus, the new vector $\hat{\boldsymbol{y}}_k^{(2)}$ which is the input of the second cycle of CEFM-GA detection for the kth user is defined as

$$\hat{\boldsymbol{y}}_k^{(2)}=[\hat{y}_k^{(2)}(1), \hat{y}_k^{(2)}(2), \cdots, \hat{y}_k^{(2)}(q)], \quad (29)$$

where $k\in\{1, 2, ..., K\}$, $q\in\{1, 2, ..., Q\}$, and the superscript (2) denotes the second cycle of CEFM-GA detection.

In the second cycle of CEFM-GA detection, the greater number of generations G' and/or the population size P' can be adopted due to the much smaller number of elements in $\hat{\boldsymbol{y}}_k^{(2)}$ (we will discuss the difference in elements rate between $\hat{\boldsymbol{y}}_k^{(2)}$ and $\boldsymbol{y}_k$ in the next section; usually it is about 10%). In our proposed CEFM-GA DA, we increase only the number of generations G'. While increasing the number of generations, our proposed MUD can also obtain better BER performance.

After the second cycle of CEFM-GA detection, $\vec{\boldsymbol{b}}_k^{(2)}$ can be obtained at the output of the major CEFM-GA detector, and then be forwarded to the DA. In the DA, a new detection result $\breve{\boldsymbol{b}}_k^{(2)}$ is formed by a replacement operation; namely, the non-zero elements in $\hat{\boldsymbol{b}}_k^{(1)}$ are replaced by the elements in $\vec{\boldsymbol{b}}_k^{(2)}$ in turn. Thus, the final results $\hat{\boldsymbol{b}}$ of the CEFM-GA DA can be expressed as

$$\hat{\boldsymbol{b}}=\vec{\boldsymbol{b}}^{(1)}-\hat{\boldsymbol{b}}^{(1)}+\breve{\boldsymbol{b}}^{(2)}=\frac{\vec{\boldsymbol{b}}^{(1)}+\tilde{\boldsymbol{b}}^{(1)}}{2}+\breve{\boldsymbol{b}}^{(2)}. \quad (30)$$

Here, we employ a two-cycled CEFM-GA with the differential algorithm (CEFM-GA DA). More cycles could be employed, if required.

Quantitative analysis can be used to compare the computational complexity of different MUDs. Thus, we used the float-point (flop) operation method (Nahler *et al*., 2002) and defined addition and multiplication operations (ops) as add and mul, respectively. The complexity O, measured as the number of ops, was calculated for successive interference

cancellation (SIC), parallel interference cancellation (PIC), conventional GA without CEFM, CEFM-GA, and CEFM-GA DA detection:

$$\begin{aligned} O(\text{SIC}) &= K[2N_\text{s}+2+(2N_\text{s}K^2+2K-1+1)] \\ &= 2K(N_\text{s}K^2+N_\text{s}+K+1), \end{aligned} \tag{31}$$

$$\begin{aligned} O(\text{PIC}) &= S\{K+N_\text{s}[K+K(K-1)]+K(2N_\text{s}-1+1)\} \\ &= SK(N_\text{s}K+2N_\text{s}+1), \end{aligned} \tag{32}$$

$$\begin{aligned} O(\text{GA}) &= G\{(3P+1)[K(K+K-1)+(K+K-1) \\ &\quad +1+3K(K+K-1)+(K+K-1)+1] \\ &\quad +6P+P_\text{mu}P+4\} \\ &= G(24PK^2+8K^2+6P+P_\text{mu}P+4), \end{aligned} \tag{33}$$

$$\begin{aligned} &O(\text{CEFM-GA}) \\ &= G\{(3P+1)[K(K+K-1)+(K+K-1) \\ &\quad +1+3K(K+K-1)+(K+K-1)+1] \\ &\quad +6P+P_\text{m}P+7\} \\ &= G(24PK^2+8K^2+6P+P_\text{m}P+7), \end{aligned} \tag{34}$$

$$\begin{aligned} &O(\text{CEFM-GA DA}) \\ &= (G_1+1)(24PK^2+8K^2+6P+P_\text{m}P+7) \\ &\quad +\beta G'(24PK^2+8K^2+6P+P_\text{m}P+7) \\ &= (\alpha G+\beta G'+1)(24PK^2+8K^2+6P \\ &\quad +P_\text{m}P+7), \end{aligned} \tag{35}$$

where K is the number of users, N_s the length of spreading code, S the number of stages in PIC, P the number of populations in the conventional GA, CEFM-GA, and CEFM-GA DA, G the number of generations in the conventional GA and CEFM-GA, P_mu the mutation probability in the conventional GA, P_m the proposed CEFM probability in our proposed CEFM-GA and CEFM-GA DA, $G_1=\alpha G$ ($0<\alpha<1/2$) the number of generations in the major detector of the CEFM-GA DA, G' the number of generations in the second cycle of CEFM-GA DA detection, and β (usually about 10%) the percentage of non-zeros in the differential matrix. Clearly, O(CEFM-GA DA)< O(CEFM-GA).

4 Simulation results

Simulations were conducted to evaluate the performance of our proposed CEFM-GA DA MUD for a multiuser UWB communication system in which direct sequence was employed. The UWB pulse was the second derivative of Gaussian pulse (Li and Rusch, 2002), as shown in Eq. (3). There were four users in the UWB system, and the length of the spreading code was 31 (Gold codes were used). The details of the system parameters are summarized in Table 1.

Table 1 Summary of system parameters

Config.	Parameter	Value/Description
GA	Population size	15
	Number of generations	
	CEFM-GA	G is varied
	Major detector of CEFM-GA DA	$G_1=\alpha G$ (α=0.3)
	Accessorial detector of CEFM-GA DA	1
	Second cycle of CEFM -GA DA	G' is varied
	Selection method	Fitness-based
	Crossover	Uniform
	Mutation	CEFM
	Elitism	Enabled
UWB	Number of users	4
	Modulation	BPSK
	Channel model	lognormal fading CM1–CM4
LDPC	Code rate	1/2
	Number of iterations	10
	Codeword length	512 bits

GA: genetic algorithm; UWB: ultra-wideband; LDPC: low-density parity-check. CEFM: complementary error function mutation; DA: differential algorithm; CM: channel model

In this article, we consider the UWB channel models (CM) of IEEE 802.15.3a CM1–CM4 (line-of-sight (LOS) and non-line-of-sight (NLOS) channel characteristics) (Foerster, 2003; Molisch *et al*., 2003) in which the channel impulse response (CIR) for each user is selected randomly from 200 channel realizations (Tan *et al.*, 2006; Ahmed and Yang, 2010). The parameters of CM1–CM4 are summarized in Table 2.

In Table 2, the mean excess delay τ_m and the root mean squared delay τ_RMS can be defined as

$$\tau_\text{m} = \sum_i \overline{P(\tau_i)}\tau_i \Big/ \sum_i \overline{P(\tau_i)}, \tag{36}$$

$$\tau_\text{RMS} = \sqrt{\sum_i \overline{P(\tau_i)}(\tau_i-\tau_\text{m})^2 \Big/ \sum_i \overline{P(\tau_i)}}, \tag{37}$$

Table 2 IEEE 802.15 UWB channel for four scenarios

Parameter	Value			
	CM1*	CM2**	CM3**	CM4**
Λ (1/ns)	0.0233	0.4000	0.0667	0.0667
λ (1/ns)	2.5	0.5	2.1	2.1
Γ	7.1	5.5	14.0	24.0
γ	4.3	6.7	7.9	12
τ_m (ns)	5.0	9.9	15.9	30.1
τ_{RMS} (ns)	5	8	15	25
$NP_{10\,dB}$	12.5	15.3	24.9	41.2
$NP_{85\%}$	20.8	33.9	64.7	123.3

* Line-of-sight (LOS); ** Non-line-of-sight (NLOS). Λ: cluster arrival rate; λ: ray arrival rate; Γ: cluster decay factor; γ: ray decay factor; τ_m: mean excess delay; τ_{RMS}: root mean squared delay; $NP_{10\,dB}$: the number of multipath arrivals that are within 10 dB of the peak multipath arrival; $NP_{85\%}$: the number of paths required to meet the 85% energy capture threshold

where τ_i denotes the delay of the ith ray and $\overline{P(\tau_i)}$ denotes the power of the ith ray (Ahmadi-Shokouh and Qiu, 2009). $NP_{10\,dB}$ is defined as the number of multipath arrivals that are within 10 dB of the peak multipath arrival, and $NP_{85\%}$ is defined as the number of paths required to meet the 85% energy capture threshold (Foerster, 2003). The definitions of the other parameters of the channel model can be found above. Note that in CM1–CM4 the channel coefficients are lognormal fading (see Eqs. (5)–(7)). Thus, the IEEE 802.15.3a UWB channel characteristic is lognormal fading (Foerster, 2003).

Fig. 4a compares the BER performance of different MUDs for the lognormal fading UWB system in CM 1 (i.e., LOS channel), where four users and a processing gain of N_s=31 are supported. Our proposed CEFM-GA and CEFM-GA DA are much better than SIC, PIC (50 stages), and conventional GA without CEFM. Specifically, G is the number of generations in CEFM-GA, and G' is the number of generations for the second cycle of detection in CEFM-GA DA (as G=10, the number of generations of the major detector $G_1=\alpha G=0.3\times10=3$). The CEFM-GA DA with G'=20 or 30 can obtain better BER performance than the CEFM-GA with G=10 (Fig. 4a), though CEFM-GA DA with G'=10 has almost the same BER performance as CEFM-GA with G=10. Concretely, at a BER of nearly 10^{-4}, the CEFM-GA DA with G'=20 attains gains of more than 1 dB and 0.5 dB compared to conventional GA and CEFM-GA, respectively. Furthermore, as G' is increased from 20 to 30, the CEFM-GA DA can provide a further gain of more than 0.5 dB.

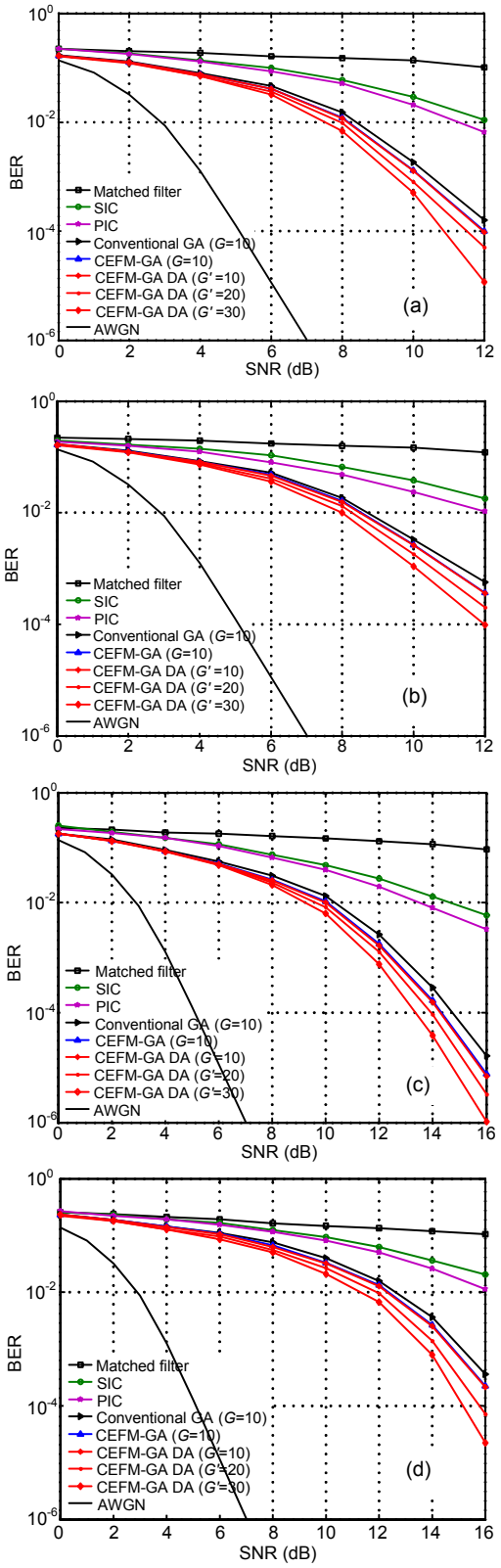

Fig. 4 BER performance of different MUDs for a lognormal fading UWB system in CM1 (a), CM2 (b), CM3 (c), and CM4 (d), where four users and a processing gain of N_s=31 are supported

Figs. 4b–4d show the BER performance of different MUDs for the lognormal fading UWB system in CM2–CM4 (i.e., NLOS channel). In Fig. 4, with the increase of cluster decay factor Γ and ray decay factor γ (see Table 2), the BER performance of all MUDs declined. But the proposed CEFM-GA DA with G'=30 had the best BER performance among all MUDs, and was closest to the performance over the AWGN channel. Figs. 4b–4d show that the CEFM-GA DA with G'=20 or 30 can obtain better BER performance than the CEFM-GA with G=10, though the CEFM-GA DA with G'=10 had almost the same BER performance as the CEFM-GA with G=10. Obviously, as G' is increased, the BER performance of CEFM-GA DA can also be improved due to the nature of the GA. But the increment of G' brings little additional computational complexity (to be discussed later).

Fig. 5 shows the percentage of non-zeros in the differential matrix (i.e., β mentioned above) for CM1–CM4, and indicates a reduction in computational complexity and an improvement in performance when the DA is used in CEFM-GA. The better are the conditions of the channel, the lower is the percentage of non-zeros in the differential matrix. Also, as the SNR is increased, the percentage of non-zeros in the differential matrix decreases slightly. The averages of the percentage of non-zeros in the differential matrix for CM1–CM4 were 9.80%, 10.07%, 10.36%, and 10.52% respectively, implying that only about 10% of data will be sent to the second cycle of detection in the CEFM-GA DA for further correction. Thus, we can save nearly 90% of computational operations in the second cycle of detection. This means that we can employ more generations (i.e., a larger G') in our algorithm to improve the BER performance (Fig. 4). The changes in the percentage of non-zeros in the differential matrix for CM1–CM4 are so tiny that they barely have any impact on the computational complexity of the whole system; therefore, we can treat the percentage of non-zeros in the differential matrix for CM1–CM4 as one fixed number, namely 10%.

Fig. 6 compares the computational complexity of different GA MUDs for different numbers of generations. We used the float-point (flop) method (Nahler *et al*., 2002) to show how many computation operations it is possible to save in a real system. The computational operations of conventional GA and

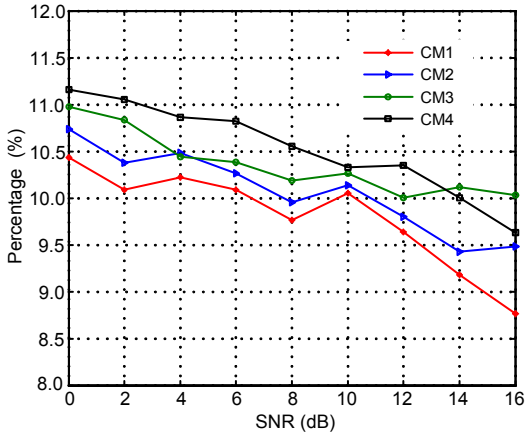

Fig. 5 Percentage of non-zeros in the differential matrix of the proposed CEFM-GA DA for CM1–CM4
The averages of the percentage of non-zeros in the differential matrix for CM1–CM4 were 9.80%, 10.07%, 10.36%, and 10.52%, respectively

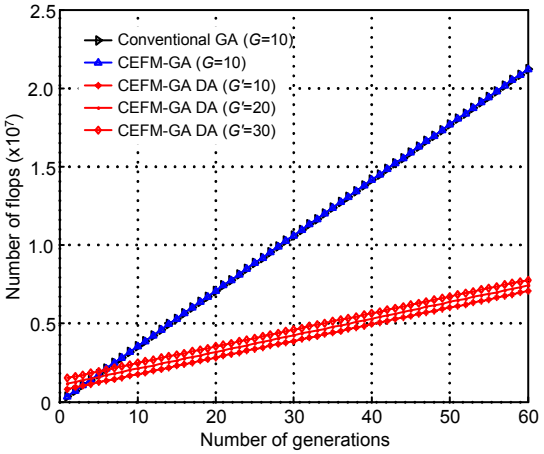

Fig. 6 Computational complexity of the proposed CEFM-GA DA compared with conventional GA and CEFM-GA for different numbers of generations

CEFM-GA increased quickly. However, the computational operations of all three proposed CEFM-GA DA increased much more slowly, and were very similar. One reason is that the number of generations G_1 of the major detector in our proposed CEFM-GA DA was set as a small number αG, namely $0.3G$. Also, the input data of the second cycle of detection, namely non-zeros in the differential matrix, formed only about 10% of the total. At G=60, the computational operations of all three proposed CEFM-GA DA were only one third of those of the conventional GA and CEFM-GA. Thus, we can employ more generations for detection by using the DA to obtain better BER performance.

Fig. 7 shows the computational complexity of different MUDs for different numbers of users. The computational operations of our proposed CEFM-GA DA with G'=10 increased the slowest. The computational operations of all three CEFM-GA DA MUDs increased slower than those of other MUDs. When the number of users was more than 16, our proposed CEFM-GA DA with G'=10 had the lowest computational complexity (Fig. 7). Thus, with our proposed CEFM-GA DA, the higher is the number of users, the lower is the system computational complexity. Figs. 6 and 7 both indicate that when we use SIC, PIC, conventional GA, or CEFM-GA, many more computational operations are wasted. Thus, we can exploit more generations for detection by using the differential algorithm to obtain better BER performance.

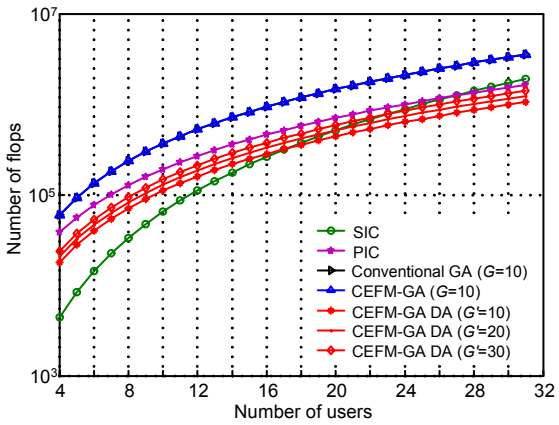

Fig. 7 Computational complexity of the proposed CEFM-GA DA compared with SIC, PIC, conventional GA, and CEFM-GA for different numbers of users

5 Conclusions

In this paper, we propose a differential multiuser detection (MUD) method with a novel genetic algorithm (GA) based on complementary error function mutation (CEFM) and a differential algorithm (DA) for UWB systems, namely CEFM-GA DA. We describe the principles of the CEFM-GA and CEFM-GA DA, give an objective function (OF) for our proposed CEFM-GA, analyze the mutation probability based on complementary error function, and employ the DA for the reduction of computational complexity and the improvement of BER performance. Compared with SIC, PIC, conventional GA, and CEFM-GA without DA, our proposed CEFM-GA DA can achieve a significant performance gain for UWB systems in lognormal fading channel. Moreover, CEFM-GA DA not only reduces computational complexity relative to conventional GA and CEFM-GA without DA, but improves BER performance.

There are still several issues that need to be investigated further, such as the GA and radial basis function (RBF) hybrid MUD and MUD for Nakagami fading cooperative UWB.

References

Ahmadi-Shokouh, J., Qiu, R.C., 2009. Ultra-wideband (UWB) communications channel measurements—a tutorial review. *Int. J. Ultra Wideband Commun. Syst.*, **1**(1):11-30. [doi:10.1504/IJUWBCS.2009.026447]

Ahmed, Q.Z., Yang, L., 2010. Reduced-rank adaptive multiuser detection in hybrid direct-sequence time-hopping ultrawide bandwidth systems. *IEEE Trans. Wirel. Commun.*, **9**(1):156-167. [doi:10.1109/TWC.2010.01.081172]

Arifianto, M.S., Chekima, A., Barukang, L., Hamid, M.Y., Viswacheda, D.V., 2007. STBC MC-CDMA with Genetic Algorithm Based MUD for Wireless Multimedia Communications. IEEE Int. Conf. on Computational Intelligence and Multimedia Applications, p.298-305. [doi:10.1109/ICCIMA.2007.345]

Biradar, G.S., Merchant, S.N., Desai, U.B., 2008. Performance of Constrained Blind Adaptive DS-CDMA UWB Multiuser Detector in Multipath Channel with Narrowband Interference. IEEE GLOBECOM, p.1-5. [doi:10.1109/GLOCOM.2008.ECP.927]

Boubaker, N., Letaief, K.B., 2004. Combined Multiuser Successive Interference Cancellation and Partial RAKE Reception for Ultra-Wideband Wireless Communications. IEEE 60th Vehicular Technology Conf., p.1209-1212. [doi:10.1109/VETECF.2004.1400214]

ECMA International, 2008. ECMA-368: High Rate Ultra Wideband PHY and MAC Standard (3rd Ed.). ECMA International, Geneva.

Foerster, J., 2003. Channel Modeling Sub-committee Report (Final). Technical Report, No. IEEE P802.15-02/490r1-SG3a. IEEE P802.15 Working Group for Wireless Personal Area Networks (WPANs), Intel R&D, OR.

Gen, M., Cheng, R., 2000. Genetic Algorithms and Engineering Optimization. John Wiley & Sons, NY.

Goldberg, D.E., 1989. Genetic Algorithms in Search, Optimization, and Machine Learning. Addison-Wesley, MA.

Hanzo, L., Keller, T., 2006. OFDM and MC-CDMA: a Primer. IEEE Press/Wiley, Piscataway, p.303-329.

Jiang, M., Hanzo, L., 2007. Multiuser MIMO-OFDM for next-generation wireless systems. *Proc. IEEE*, **95**(7):1430-1469. [doi:10.1109/JPROC.2007.898869]

Jiang, M., Ng, S.X., Hanzo, L., 2006. Hybrid iterative multiuser detection for channel coded space division multiple access OFDM systems. *IEEE Trans. Veh. Technol.*,

55(1):115-127. [doi:10.1109/TVT.2005.861187]

Kaligineedi, P., Bhargava, V.K., 2008. Frequency-domain turbo equalization and multiuser detection for DS-UWB systems. *IEEE Trans. Wirel. Commun.*, **7**(9):3280-3284. [doi:10.1109/TWC.2008.070274]

Kong, Z., Jiang, J., Zhu, G., 2008. A Study of Differencing Structure Decision Feedback Equalizer with Multiuser Feedback. IET Int. Conf. on Wireless, Mobile and Multimedia Networks, p.172-175. [doi:10.1049/cp:20080172]

Kong, Z., Zhu, G., Tong, Q., Li, Y., 2010. A novel differential multiuser detection algorithm for multiuser MIMO-OFDM systems. *J. Zhejiang Univ.-Sci. C (Comput. & Electron.)*, **11**(10):798-807. [doi:10.1631/jzus.C0910735]

Li, Q., Rusch, L.A., 2002. Multiuser detection for DS-CDMA UWB in the home environment. *IEEE J. Sel. Areas Commun.*, **20**(9):1701-1711. [doi:10.1109/JSAC.2002.805241]

Molisch, A.F., Foerster, J.R., Pendergrass, M., 2003. Channel models for ultrawideband personal area networks. *IEEE Wirel. Commun.*, **10**(6):14-21. [doi:10.1109/MWC.2003.1265848]

Nahler, A., Irmer, R., Fettweis, G., 2002. Reduced and differential parallel interference cancellation for CDMA systems. *IEEE J. Sel. Areas Commun.*, **20**(2):237-247. [doi:10.1109/49.983335]

Proakis, J.G., Salehi, M., 2007. Digital Communications (5th Ed.). McGraw-Hill, Whitby, p.88-126.

Qiu, R.C., 2005. Optimum and sub-optimum detection of physics-based ultra-wideband signals—a tutorial review. *Dyn.Contin. Discr. Impul. Syst. Ser. B*, **12**(3):321-334.

Saleh, A., Valenzuela, R., 1987. A statistical model for indoor multipath propagation. *IEEE J. Sel. Areas Commun.*, **5**(2):128-137. [doi:10.1109/JSAC.1987.1146527]

Shen, X., Guizani, M., Chen, H.H., Qiu, R.C., Molisch, A.F., 2006a. Ultrawideband wireless communications—theory and applications. *IEEE J. Sel. Areas Commun.*, **24**(4):713-716. [doi:10.1109/JSAC.2005.863805]

Shen, X., Guizani, M., Qiu, R.C., Le-Ngoc, T., 2006b. UWB Wireless Communications and Networks. IEEE Press/Wiley, Piscataway, p.37-51.

Surajudeen-Bakinde, N., Zhu, X., Gao, J., Nandi, A.K., 2009. Genetic Algorithm Based Equalization for Direct Sequence Ultra-Wideband Communications Systems. IEEE WCNC, p.1-5. [doi:10.1109/WCNC.2009.4917737]

Tan, T., Huang, Y., Lin, C., Fu, R., 2006. Performance Improvement of Multiuser Detection Using a Genetic Algorithm in DS-CDMA UWB Systems over an Extreme NLOS Multipath Channel. IEEE Int. Conf. on Systems, Man, and Cybernetics, p.1945-1950. [doi:10.1109/ICSMC.2006.385015]

Verdu, S., 1998. Multiuser Detection. Cambridge University Press, Cambridge, p.88-213.

Wen, J., Hung, H., Chao, C., Cheng, C., 2010. An Effective Hybrid GACSA-Based Multi-user Detection for Ultra-Wideband Communications Systems. IEEE WICON, p.1-7.

Yen, K., Hanzo, L., 2004. Genetic-algorithm-assisted multiuser detection in asynchronous CDMA communications. *IEEE Trans. Veh. Technol.*, **53**(5):1413-1422. [doi:10.1109/TVT.2004.832412]

Zhong, L., Zhu, G., Kong, Z., Li, Y., Huang, L., 2010. Novel Cluster Identification Algorithm for Ultra-Wide Band Channel. 6th Int. Conf. on Wireless Communications, Networking and Mobile Computing, p.1-4. [doi:10.1109/WICOM.2010.5600927]

2010 JCR of Thomson Reuters for *JZUS-A* and *JZUS-B*

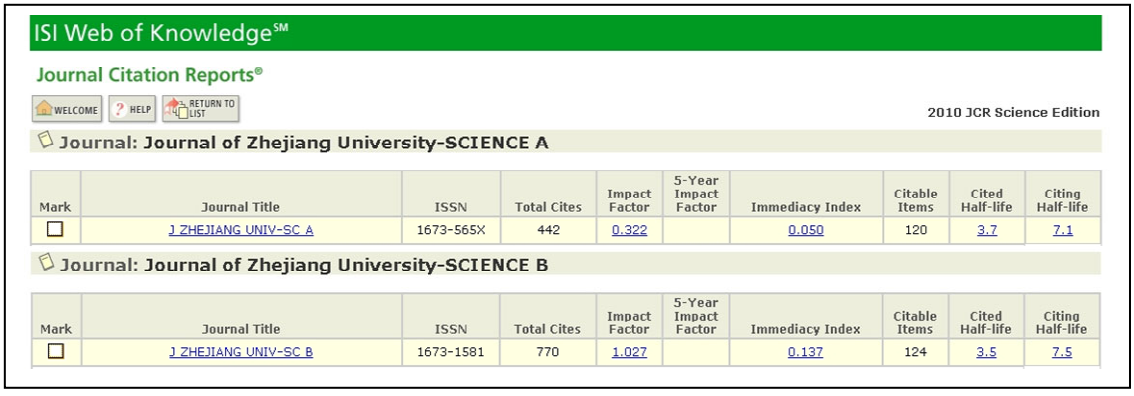

ISI Web of Knowledge℠

Journal Citation Reports®

WELCOME | HELP | RETURN TO LIST

2010 JCR Science Edition

Journal: Journal of Zhejiang University-SCIENCE A

Mark	Journal Title	ISSN	Total Cites	Impact Factor	5-Year Impact Factor	Immediacy Index	Citable Items	Cited Half-life	Citing Half-life
☐	J ZHEJIANG UNIV-SC A	1673-565X	442	0.322		0.050	120	3.7	7.1

Journal: Journal of Zhejiang University-SCIENCE B

Mark	Journal Title	ISSN	Total Cites	Impact Factor	5-Year Impact Factor	Immediacy Index	Citable Items	Cited Half-life	Citing Half-life
☐	J ZHEJIANG UNIV-SC B	1673-1581	770	1.027		0.137	124	3.5	7.5

JZUS-A is an international “Applied Physics & Engineering” reviewed-Journal, covering research in Applied Physics, Mechanical and Civil Engineering, Environmental Science and Energy, Materials Science, and Chemical Engineering. *JZUS-B* is an international “Biomedicine & Biotechnology” reviewed-Journal, covering research in Biomedicine, Biochemistry, and Biotechnology. *JZUS-A* and *JZUS-B* were covered by SCI-E in 2007 and 2008, respectively.